JOURNAL OF SOLID STATE CHEMISTRY 65, 79–88 (1986)

Ammonia Oxidation and Charge Compensation in the Metal Ammonia Intercalates $Li_x^+(NH_4^+)_{y'}(NH_3)_{y''}TiS_2^{(x+y')-}$ *

M. McKELVY, L. BERNARD, AND W. GLAUNSINGER†

Department of Chemistry, Arizona State University, Tempe, Arizona 85287

AND P. COLOMBET

Laboratoire de Chimie des Solides, L.A. 279, 2, rue de la Houssinière, 44072 Nantes Cédex, France

Received October 28, 1985; in revised form March 3, 1986

The lithium–ammonia intercalates of TiS_2, $Li_x^+(NH_4^+)_{y'}(NH_3)_{y''}TiS_2^{(x+y')-}$, where $0.00 \leq x \leq 0.20$, have been investigated by thermogravimetric analysis (TGA), vapor pressure measurements, X-ray powder diffraction, and SQUID magnetometry. TGA and vapor-pressure measurements indicate that ammonia deintercalation occurs by a distinct two-step process consistent with the ionic nature of these compounds. These materials are monophasic and crystallize in a 3R-type structure. The **c** lattice parameter increases linearly with increasing ammonia content, which may be associated with the diminution of the ion-dipole interaction of the cation(s) with the lone pair of ammonia. Compositional analysis by TGA shows that charge compensation occurs such that the total cationic concentration ($x + y'$) is constant at 0.22 ± 0.02. The Pauli paramagnetism of the conduction electrons corresponds to complete ionization of both lithium and ammonium, so that the driving force for the charge-transfer phenomenon is the transfer of 0.22 ± 0.02 electrons to the conduction band of TiS_2. The degree of NH_3 oxidation depends upon the relative intercalation rate of metal and NH_3.

Introduction

Intercalation compounds are formed by the reversible inclusion of guest species (or intercalants) into a host structure (*1*). The intercalation compounds of the lamellar transition metal disulfides, TS_2, where T is a group IV, V, or VI B transition metal, are of particular importance due to their fascinating structures and properties. The structure of the TS_2 host consists of two-dimensional [S–T–S] layers stacked one upon the other. The intralayer bonding is strong and covalent, whereas the interlayer forces are weak and of the van der Waals (VDW) type. The intercalation process is driven by a sufficiently strong guest–host interaction to overcome the relatively weak VDW forces between the host layers as well as any guest–guest interactions. Apparently, a transfer of electron density from the guest to the TS_2 host must occur during the inter-

* This research was supported by NSF Grant DMR 82-15315 and NSF-CNRS Grant C-CHE-0394.

† To whom correspondence should be addressed.

0022-4596/86 $3.00

calation process, which can be qualitatively understood from the energy-band structure of the host (*2, 3*).

A broad spectrum of Lewis bases can be intercalated into TS_2 hosts (*4*). In this regard, ammonia is the simplest Lewis base that can be intercalated into TS_2, and the resulting intercalates have been studied rather extensively. Intuitively, one might expect the NH_3 molecule to be oriented such that its C_3 axis is perpendicular to the layers, thus maximizing the degree of electron transfer from the NH_3 lone pair to the host. However, NMR studies have indicated that the C_3 axis of NH_3 is actually parallel to the host layers for nominally NH_3TaS_2 (*5*). In subsequent work, it has been demonstrated that redox reactions accompany the ammoniation of TaS_2 to form $(NH_4^+)_x(NH_3)_{1-x}TaS_2^{x-}$, where $x \simeq 0.1$ (*6*). Given a significant concentration of NH_4^+, its presence could orient the C_3 axis of neighboring NH_3 molecules such that the NH_3 lone pair is directed at NH_4^+ midway between the host layers. Recently, the authors have shown that NH_3 oxidation also occurs in ammoniated TiS_2 to yield $(NH_4^+)_{y'}(NH_3)_{y''}TiS_2^{y'-}$, where $y' \simeq 0.20$, with the primary electron transfer to the host coming from NH_4^+ rather than the NH_3 lone pair (*7*). Recently, we have found that NH_4^+ is also present in ammoniated NbS_2 (*8*), which strongly suggests that NH_3 oxidation is a general phenomenon. Hence, from the viewpoint of electron transfer, the NH_4^+ ions play the same role as alkali–metal cations M^+ in the intercalation compounds M_xTS_2.

Li_xTiS_2, where $0 < x \leq 1$, is the most extensively investigated of the M_xTiS_2 intercalation compounds due to its structural simplicity and utility as a battery cathode material (*9*). Li_xTiS_2 adopts the CdI_2 structure, with Li atoms apparently occupying interlayer octahedral sites forming a two-dimensional hexagonal network (*9*). These intercalation compounds are metallic due to the donation of Li valence-electron density to the conduction band of the host TiS_2. A ^7Li NMR investigation of Li_xTiS_2 ($0 < x \leq 1$) has suggested that the transfer of the Li 2*s* electron to the host is essentially complete for small x, whereas for $Li_{1.0}TiS_2$ only about 85% of the Li 2*s* electron density is transferred to the host (*10*). Recent magnetic susceptibility measurements confirm this finding (*11*). In addition to being a good electronic conductor, Li_xTiS_2 is also a good ionic conductor (*12*). Intriguing structural features in Li_xTiS_2 are observed as anomalies in voltage-composition curves, which have been attributed by different workers to intralayer and/or interlayer ordering of the Li^+ ions (*13–18*).

Relatively few M–NH_3 intercalation complexes, $M_x(NH_3)_yTS_2$, have been investigated (*19–21*), even though these materials are well-known intermediates in the synthesis of M_xTS_2 by the liquid-ammonia technique. The paucity of information on such mixed-guest intercalation compounds, as well as the highly unusual structures and properties of M–NH_3 compounds (*22*), has motivated us to undertake a comprehensive program to investigate these materials. Below we report and discuss our results for Li and NH_3 intercalated into TiS_2 by the liquid-ammonia technique.

Experimental

TiS_2 was obtained by direct reaction of the elements (*23*). The titanium wire (Materials Research Corporation) had a stated purity of 99.93%, with O (500 ppm), Fe (50 ppm), Ni (30 ppm), and C (30 ppm) being the major impurities. The stated purity of the sulfur (Aldrich Chemical Company) was 99.999%, and Fe (0.1–0.5 ppm) and Si (0.1–0.5 ppm) were the major impurities. TiS_2 was synthesized in sealed, evacuated (10^{-4} Torr) quartz ampoules at 640°C. The product was ground in a Vacuum Atmospheres Model MO-40-1H Dri-Train glove-

box ($\lesssim$1 ppm H_2O and O_2) using He as the inert gas. The TiS_2 was then reheated to 640°C in a similar quartz ampoule with 40 mg/cm^3 excess sulfur to attain stoichiometry. The ampoule was subsequently water quenched to avoid TiS_3 formation (*24*), and excess sulfur was removed by vapor transport. The TiS_2 stoichiometry was determined by measuring the ammonia intercalation time, magnetic susceptibility, and total mass loss upon oxidation of TiS_2 to TiO_2 in oxygen at 900°C using a computer-controlled Perkin-Elmer TGS-2 thermogravimetric analysis (TGA) system.

Lithium (99.9% ROC/RIC) was loaded into one leg of a Pyrex "h" tube with TiS_2 in the opposite leg. Ammonia (99.9% Matheson Gas Products), was dried over sodium and then cryopumped slowly into the lithium-containing leg of the "h" tube, with the "h" tube then sealed to form a "n" tube. The NH_3 was in large excess of its maximum 1 : 1 stoichiometry with TiS_2. The Li–NH_3 solution was then poured onto the TiS_2 at 20°C, and the solution turned colorless in a minute or less, which signaled that the intercalation of Li was complete. The reaction tubes were still allowed to sit overnight to further ensure complete reaction. Most of the exess NH_3 was poured into the opposite leg of the "n" tube, with the remainder being cryopumped, and this leg was sealed off. The leg containing the product was broken in the glovebox, and the samples were stored in weighing bottles placed in sealed Ball jars. This procedure greatly retarded the problematic NH_3 volatilization from these compounds (*7*), since an equilibrium NH_3 pressure is established within the jar and NH_3 is lost only when the jar is opened briefly to remove a sample. Ammoniated TiS_2 was prepared using the same procedure, and about 2 hr was required for complete intercalation (*7*). Both TiS_2 and the intercalates were always handled in the glovebox and only transferred from the glovebox in sealed containers. These containers were tested with P_2O_5, $Li_{0.5}TiS_2$, and sodium metal to ensure adquate seals. Although TiS_2 is only mildly air sensitive (*25*), its Li–NH_3 intercalates are extremely air sensitive, so that the above precautions were essential for reliable experiments.

The NH_3 and NH_4^+ stoichiometry was determined by TGA for all samples and by vapor-pressure measurements (*7*) for selected samples. For the TGA experiments, temperatures were calibrated to ±2°C using magnetic transition standards located in a magnetic field, and NBS standard weights were used to calibrate the mass measurements (sensitivity = 0.1 μg). Samples were hermetically sealed in aluminum sample pans using a Perkin-Elmer volatile-sample-pan sealing press in the glovebox and transferred to a glovebox surrounding the TGS-2, which was then flushed with argon (99.995%) in the presence of dry P_2O_5. A very small pinhole was made in the pan just prior to loading samples into the TGA setup to facilitate NH_3 and H_2 escape during analysis. Argon (99.999% Matheson Gas Products) was further purified by passage through a R. D. Mathis GP-100 inert-gas purifier and subsequently used as the TGA carrier gas at a flow rate of 40 cm^3/min. The optimum heating rate was 2°C/min. After analysis, selected pans were opened and examined microscopically to verify that no reaction between the compound and pan had occurred. In all cases, the aluminum surface remained smooth and silvery.

Vapor-pressure measurements were made using a glass vacuum line equipped with a Baratron gauge. The line was evacuated to 10^{-5} Torr, and samples were heated slowly. Both NH_3 and NH_4^+ could be completely deintercalated by heating to about 250°C.

X-ray samples were loaded into 0.3-mm pyrex capillaries in the glovebox, sealed with an ultratorr fitting (Cajon Company), removed from the glovebox, and then

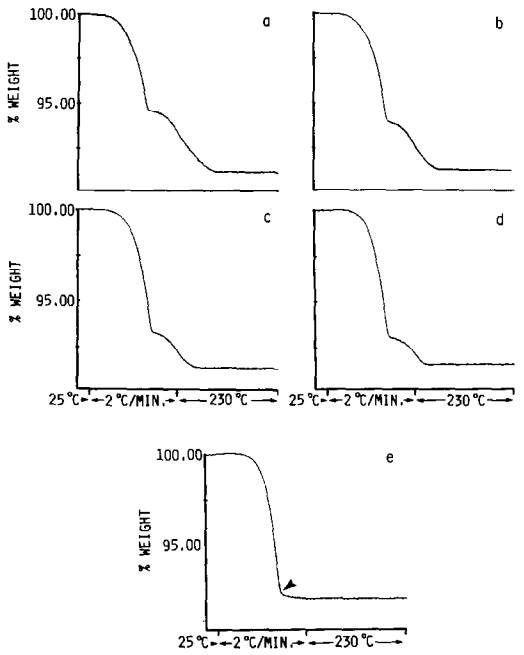

FIG. 1. Typical TGA curves of $Li_x^+(NH_4^+)_{y'}(NH_3)_{y''}TiS_2^{(x+y')-}$ for $x = 0.00$ (a), $x = 0.04$ (b), $x = 0.08$ (c), $x = 0.11$ (d), and $x = 0.20$ (e). The low- and high-temperature steps originate from the deintercalation of NH_3 and NH_4^+, respectively, according to reactions (3) and (4).

sealed with a torch under an atmosphere of helium. Again, this procedure was necessary to preserve the integrity of the samples. X-ray powder diffraction patterns were recorded at ambient temperature using Ni-filtered Cu$K\alpha$ radiation and a Debye Scherrer camera previously calibrated with NBS SRM 640 silicon. X-ray samples were rerun several days to weeks later to confirm that the capillaries were adequately sealed. Cu$K\alpha_1$ and Cu$K\alpha_2$ reflections were observed for $d \lesssim 1.00$ Å, in which case the observed d spacing was calculated from the Cu$K\alpha_1$ reflections.

The magnetic susceptibility (χ) was measured using a SHE Model VTS -905 SQUID Magnetometer having a maximum field of 25 kG and sensitivity of 10^{-12} emu/g. The NBS standards Pt and Pd were used to calibrate χ, and sample temperatures were calibrated using germanium and platinum resistance thermometers and the magnetic alloy $PdTb_3$. Large samples (100–150 mg) were sealed in Delrin buckets in the glovebox. Each bucket had a threaded top that was sealed with a thin layer of silicone grease prior to its removal from the glovebox and subsequent loading into the magnetometer.

Results and Discussion

TiS_2 Characterization

The stoichiometry of the host was found to be $Ti_{1.003\pm.001}S_2$ by TGA. Both χ (9×10^{-6} emu/mole) and ammonia intercalation time (intercalation is complete in ≃2.2 hr at 20°C) indicate that TiS_2 is essentially "stoichiometric" (*26*). The ammonia intercalation time is very sensitive to excess Ti, since it resides in the VDW gap and serves to pin the [S–*T*–S] layers together, which causes a dramatic increase in intercalation time (*26*).

Thermal Analysis

Five lithium compositions were investigated for the $Li_x^+(NH_4^+)_{y'}(NH_3)_{y''}TiS_2^{(x+y')-}$ complexes: $x = 0.00$, 0.04, 0.08, 0.11, and 0.20. A typical TGA curve for each composition and the corresponding compositional data are shown in Fig. 1 and Table I, respectively. Both y' and y'' can be determined to ±0.01 from the mass loss. Two

TABLE I

COMPOSITION OF $Li_x^+(NH_4^+)_{y'}(NH_3)_{y''}TiS_2^{(x+y')-}$ INTERCALATION COMPOUNDS DERIVED FROM THE TGA CURVES IN FIG. 1

Compound	$x + y'$	$y' + y''$
$(NH_4^+)_{0.23}(NH_3)_{0.39}TiS_2^{0.23-}$	0.23	0.62
$Li_{0.04}^+(NH_4^+)_{0.18}(NH_3)_{0.43}TiS_2^{0.22-}$	0.22	0.61
$Li_{0.08}^+(NH_4^+)_{0.14}(NH_3)_{0.48}TiS_2^{0.22-}$	0.22	0.62
$Li_{0.11}^+(NH_4^+)_{0.11}(NH_3)_{0.50}TiS_2^{0.22-}$	0.22	0.61
$Li_{0.20}^+(NH_4^+)_{0.02}(NH_3)_{0.56}TiS_2^{0.22-}$	0.22	0.58

distinct steps are resolved for each of the curves in Fig. 1. The authors have shown previously by TGA, vapor-pressure measurements, and chemical analysis that for $x = 0.00$ the reactions that correspond to steps I and II are as follows (*7*):

$$\text{Step (I):}\quad (NH_4^+)_{y'}(NH_3)_{y''}TiS_2^{y'-} \rightarrow (NH_4^+)_{y'}TiS_2^{y'-} + y''NH_3 \quad (1)$$

$$\text{Step (II):}\quad (NH_4^+)_{y'}TiS_2^{y'-} \rightarrow TiS_2 + y'NH_3 + \frac{y'}{2}H_2. \quad (2)$$

To determine the nature of the evolved gases for the Li–NH_3 intercalates, the vapor pressure was measured as a function of the temperature for selected $Li_x^+(NH_4^+)_{y'}(NH_3)_{y''}TiS_2^{(x+y')-}$ samples. Two steps were displayed in the resulting pressure vs temperature curves which coincided with the TGA curves in Fig. 1 within experimental error. The gas evolved in the first step was completely condensable at liquid-nitrogen temperature, whereas only two-thirds of the gas evolved in the second step could be condensed under the same conditions. The condensable gas was identified as NH_3, and the authors have shown previously that the noncondensable gas is H_2 (*7*). Furthermore, the $Li_x^+(NH_4^+)_{y'}(NH_3)_{y''}TiS_2^{(x+y')-}$ stoichiometry determined by vapor-pressure measurements was in good agreement with that determined by TGA provided the H_2 pressure in reaction (2) is taken into account. Hence, reactions (1) and (2) can be generalized to the Li–NH_3 intercalates ($0.00 \leq x \leq 0.20$) as well:

$$\text{Step (I):}\quad Li_x^+(NH_4^+)_{y'}(NH_3)_{y''}TiS_2^{(x+y')-} \rightarrow Li_x^+(NH_4^+)_{y'}TiS_2^{(x+y')-} + y''NH_3 \quad (3)$$

$$\text{Step (II):}\quad Li_x^+(NH_4^+)_{y'}TiS_2^{(x+y')-} \rightarrow Li_x^+TiS_2^{x-} + y'NH_3 + \frac{y'}{2}H_2. \quad (4)$$

From Table I it follows that the ammonium mole fraction y' decreases as the lithium mole fraction x increases such that their sum is constant, i.e., $x + y' = 0.22 \pm 0.01$. This result is in excellent agreement with several different $(NH_4^+)_{y'}(NH_3)_{y''}TiS_2^{y'-}$ preparations, which yielded $y' = 0.22 \pm 0.02$ by TGA. In a subsequent section, we demonstrate that both the lithium and ammonium are essentially completely ionized, so that charge compensation occurs during the formation of $Li_x^+(NH_4^+)_{y'}(NH_3)_{y''}TiS_2^{(x+y')-}$ in the compositional range $0 < x \leq 0.20$.

TABLE II

CELL CONSTANTS OF $Li_x^+(NH_4^+)_{y'}(NH_3)_{y''}TiS_2^{(x+y')-}$ FOR $0.00 \leq x \leq 0.20$[a]

Compound	a (Å)	c (Å)
$(NH_4^+)_{0.24}(NH_3)_{0.32}TiS_2^{0.24-}$	3.420	26.12
$Li_{0.04}^+(NH_4^+)_{0.18}(NH_3)_{0.41}TiS_2^{0.22-}$	3.424	26.35
$Li_{0.08}^+(NH_4^+)_{0.14}(NH_3)_{0.47}TiS_2^{0.22-}$	3.421	26.46
$Li_{0.11}^+(NH_4^+)_{0.11}(NH_3)_{0.50}TiS_2^{0.22-}$	3.423	26.48
$Li_{0.20}^+(NH_4^+)_{0.02}(NH_3)_{0.58}TiS_2^{0.22-}$	3.424	26.71

[a] The experimental uncertainties in **a** and **c** are ±0.003 and ±0.02 Å, respectively.

X-ray Analysis and Structure

TiS_2 possesses the single-layer trigonal structure (1T) with Ti octahedrally coordinated to sulfur. During intercalation it is not uncommon for the stacking sequence of the [S–*T*–S] layers to rearrange. The data shown in Table II are in good agreement with a three-layer, 3R-type structure in which such a rearrangement has occurred. The hexagonal lattice constants were determined by a least-squares refinement of the data.

Previously, the authors were unable to obtain monophasic-3R stage I-ammoniated TiS_2, but rather only mixtures of stage I and II (*7*). However, by tightly sealing these materials, thereby greatly reducing the NH_3 loss with time, a single-phase stage I structure was found, in agreement with previous work on nominally NH_3TiS_2 (*27*). The mixed-stage structures probably originated

TABLE III

POWDER X-RAY DATA FOR $Li^{+}_{0.08}(NH^{+}_{4})_{0.14}(NH_3)_{0.47}TiS^{0.22-}_{2}$ [a]

(hkl)	d_{calc} (Å)	d_{obs} (Å)	I	(hkl)	d_{calc} (Å)	d_{obs} (Å)	I
003	8.82	8.84	vs	2,0,11	1.261	1.262	vvw
006	4.410	4.407	w	1,0,19	1.260		
009	2.940	2.939	vw	1,1,15	1.228	1.228	vw
012	2.891	2.889	w	0,2,13	1.198	1.198	vw
104	2.704	2.703	vw	122	1.116		
015	2.585	2.585	s	1,1,18	1.115	1.115	vw
107	2.332	2.327	vw	1,0,22	1.114		
018	2.207	2.206	w	125	1.096	1.096	w
1,0,10	1.974	1.975	w	128	1.061	1.061	vw
0,1,11	1.867	1.864	vw	2,1,10	1.031	1.031	vw
0,0,15	1.764	1.766	vw	300	0.9877	0.9880	vw
110	1.711	1.710	mw	2,1,13	0.9812	0.9810	vw
113	1.679	1.677	mw	220	0.8554	0.8551	vw
1,0,13	1.678			1,0,31	0.8201		
202	1.472	1.472	vw	3,0,18	0.8198	0.8198	vvw
205	1.427	1.426	w	2,1,22	0.8196		
208	1.352	1.353	vw	315	0.8121	0.8118	vw
0,2,10	1.293	1.293	vw	318	0.7975	0.7975	vvw
				1,3,10	0.7848	0.7852	vvw

[a] The X-ray data for the other compounds in Table II are available in M. McKelvy, Ph.D. thesis, Arizona State University, 1985.

from the relatively rapid loss of NH_3 from these compounds with time, since exposure of nominally NH_3TiS_2 to a vacuum at ambient temperature has been reported to produce rapidly the stage II compound (*28*).

All of the observed diffraction lines could be indexed to the unit cells in Table II, with the exception of a very weak, diffuse line at ≈7.4 Å for $Li^{+}_{0.04}(NH^{+}_{4})_{0.18}(NH_3)_{0.41}TiS^{0.22-}_{2}$. This line can be identified as a stage II reflection, in good agreement with work on ammoniated TiS_2 (*4*, *7*). Since this line was <3% of the intensity of the strongest reflection, which was (003), we estimate this intercalate to be almost entirely single phase (3R), while the remaining compounds are single phase (3R) within the resolution of the X-ray data. The X-ray data for $Li^{+}_{0.08}(NH^{+}_{4})_{0.14}(NH_3)_{0.47}TiS^{0.22-}_{2}$ is shown in Table III and is typical of these compounds. Not only do all five intercalates index to 3R structures, but the relative intensities of their individual reflections are also very similar. Therefore, these materials lie within a single-phase region of the tenary phase diagram for $0.00 \leq x \leq 0.20$ and $y' + y'' \simeq 0.60$.

Within this single-phase region there is a lattice expansion in the **c** direction with increasing lithium content. Since the radii for Li^+, Li, NH^+_4, and NH_3 are 0.7, 1.4, ≈1.43 (*29*), and 1.67 Å,[1] respectively, and the expansions measured experimentally range from 3.01 to 3.21 Å on intercalation, it appears that NH_3 is the primary species responsible for the expansion. A plot of the NH_3 mole fraction (y'') versus the **c** lattice

[1] This value is derived by taking one-half the nearest-neighbor NH_3 distance in solid NH_3. The NH_3 radius estimated from the VDW radii of N and H is ≈1.6 Å.

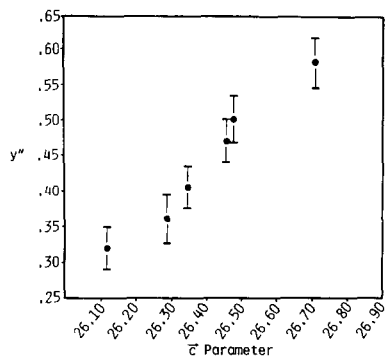

FIG. 2. Variation of **c** parameter with ammonia content (y'') in $Li_x^+(NH_4^+)_{y'}(NH_3)_{y''}TiS_2^{(x+y')-}$, where $x + y' = 0.22 \pm 0.02$. The data points correspond to $Li_x^+(NH_4^+)_{y'}(NH_3)_{y''}TiS_2^{(x+y')-}$ in Table II and $(NH_4^+)_{0.24}(NH_3)_{0.36}TiS_2^{0.24-}$.

parameter in Fig. 2 reveals a linear increase in **c** with increasing NH_3 mole fraction within experimental error. Previous NMR studies have shown that the C_3 axis of ammonia lies parallel to the host layers in ammoniated TaS_2 and TiS_2 (*5, 28*). Using this model for Li–NH_3 intercalants, the observed lattice expansion may be due to decreased ion–dipole interactions. Since the cation concentration between the layers is constant ($x + y' = 0.22 \pm .02$), as more ammonia is introduced between the layers less electron density per NH_3 is transferred to the cation(s) via ion–dipole interactions resulting in an increase in the effective size of NH_3.

Although the **c** parameter increases by more than 2% for increasing x, the **a** parameter is constant within experimental error. The **a** parameter expansion on intercalation of TiS_2 increases with increasing electron density in the TiS_2 layer (*30*). For example, **a** = 3.407 Å for TiS_2, whereas **a** = 3.454 Å for $LiTiS_2$, where ≃0.85 el/Li atom are donated to the TiS_2 host (*10, 11, 30*). Therefore, the constant **a** parameter for these intercalates suggests that they have the same electron density in the TiS_2 layers within experimental error. This result is in agreement with the thermal analysis studies and is verified quantitatively by the magnetic measurements discussed below.

Magnetic Measurements

Due to the small susceptibility of TiS_2 as well as the intercalation compounds studied here, paramagnetic impurities normally make an important contribution to χ at low temperatures, as evidenced by the pronounced Curie tail shown in Fig. 3. At 4.2 K, the magnetization (M) is not a linear function of the magnetic field (H) at higher fields, and the Curie contribution to χ agrees quite well with a Brillouin function for $J = \frac{5}{2}$. Since Fe is the major magnetic impurity in the titanium wire used in the TiS_2 synthesis, the primary impurity is probably Fe^{3+}. The absence of ferromagnetic impurities was demonstrated by the reversibility of the M vs H curves at all temperatures.

Variable-temperature magnetic studies were carried out at 25 kG. Above about 25 K, all of the M vs H plots were linear up to 25 kG within experimental error, so that $\chi = M/H$. However, below 25 K the M vs H plots were not linear, and the low-field susceptibility was determined using a Brillouin function for $J = \frac{5}{2}$.

The intrinsic susceptibility for $Li_x^+(NH_4^+)_{y'}(NH_3)_{y''}TiS_2^{(x+y')-}$ per mole of Ti was obtained after correction for the paramag-

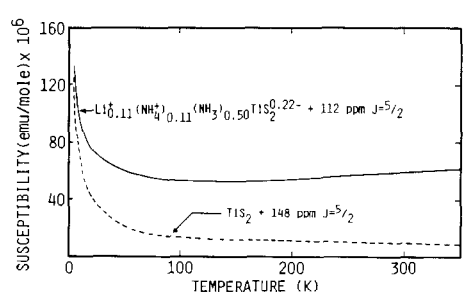

FIG. 3. The temperature dependence of the magnetic susceptibility of TiS_2 and $Li_{0.11}^+(NH_4^+)_{0.11}(NH_3)_{0.50}TiS_2^{0.22-}$. The low-temperature Curie tail can be fit to a paramagnetic species having $J = \frac{5}{2}$ (not shown).

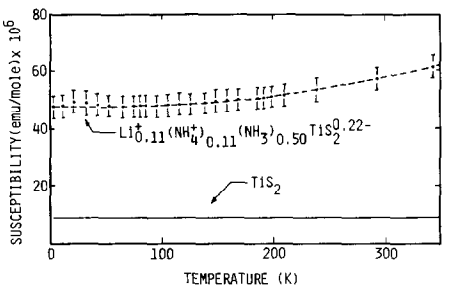

FIG. 4. The intrinsic magnetic susceptibility of TiS_2 and $Li^+_{0.11}(NH^+_4)_{0.11}(NH_3)_{0.50}TiS_2^{0.22-}$ as a function of temperature.

netic impurity contribution, as illustrated in Fig. 4. TiS_2 displays a small temperature-independent susceptibility of 9×10^{-6} emu/mole, which does not change after intercalation and deintercalation of NH_3 (*7, 26*). Below about 100 K, $Li^+_x(NH^+_4)_{y'}(NH_3)_{y''}TiS_2^{(x+y')-}$ exhibits a considerably higher temperature-independent paramagnetism than TiS_2. This observation is in accord with the expected metallic behavior arising from the transfer of electrons from the intercalant to the titanium t_{2g} conduction band, as found previously for K_xTiS_2 (*31*), $LiTiS_2$ (*32*), and ammoniated TiS_2 (*7*). The effect of electron transfer from guest to host is depicted in Fig. 5, where we have assumed that the band structure of the host TiS_2 is not perturbed by the intercalant, so that the rigid-band model is valid. The increase in the intrinsic susceptibility with temperature above 100 K may be due to an increased conduction electron concentration resulting from thermal excitation (*11*).

Within the rigid-band model, the intrinsic susceptibility of $Li^+_x(NH^+_4)_{y'}(NH_3)_{y''}TiS_2^{(x+y')-}$ can be written as follows:

$$\chi = \chi_{TiS_2} + \chi_d + \chi_p, \qquad (5)$$

where χ_{TiS_2} is the host TiS_2 susceptibility (9×10^{-6} emu/mole) (*7*), χ_d is the diamagnetic correction for ammonia (-15.8×10^{-6} emu/mole) (*33*) and Li^+ (-0.6×10^{-6} emu/mole), and χ_p is the Pauli paramagnetism of the conduction electrons, which is proportional to the density of electronic states in the conduction band. Below about 100 K, χ_p was found to be constant within experimental error for all of the compounds. The low-temperature χ_p values for the intercalates are compared to that for $Li_{0.2}TiS_2$ in Table IV. In $Li_{0.2}TiS_2$, the transfer of the Li 2*s* electron to the host is essentially complete (*10*). Since χ_p of $Li^+_x(NH^+_4)_{y'}(NH_3)_{y''}TiS_2^{(x+y')-}$ for $0.00 \leq x \leq 0.20$ is the same as for $Li_{0.2}TiS_2$ within experimental error, we conclude that for each compound NH_3 is oxidized to the extent necessary to transfer a total of 0.22 ± 0.02 mole of electrons per mole of TiS_2 to the host conduction band. Apparently, at this critical electron concentration the chemical potential of NH_3 is equal to that of the reduced host, so that no further NH_3 oxidation occurs. Also listed in Table IV is χ_p per mole of cation, $\chi'_p = \chi_p/(x + y')$, which accounts for the small cationic concentration differences. In this case there is even better agreement among the data for different compounds. The essentially identical magnetic behavior among these materials is further demonstrated by comparing their χ'_p vs temperature relationships, as shown in Fig. 6. The invariance of χ'_p shows that the guest-to-host electronic transfer is the same for each of these compounds ($x + y' = 0.22 \pm 0.02$), which demonstrates the quantitative nature of the charge-compensation process.

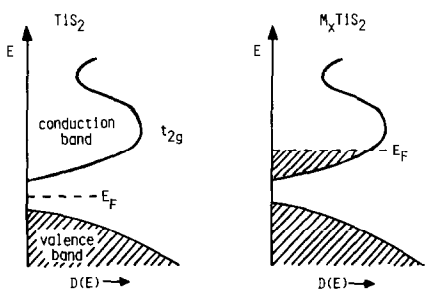

FIG. 5. Schematic energy-band diagrams of TiS_2 and M_xTiS_2 assuming the rigid-band model.

TABLE IV

LOW-TEMPERATURE MAGNETIC SUSCEPTIBILITIES OF $Li_x^+(NH_4^+)_{y'}(NH_3)_{y''}TiS_2^{(x+y')-}$ AND $Li_{0.20}^+TiS_2^{0.20-}$

Compound[a]	$x + y'$	$\chi_P \times 10^{-6}$ emu/mole[b]	$\chi_P' \times 10^{-6}$ emu/mole[c]
$(NH_4^+)_{0.20}(NH_3)_{0.28}TiS_2^{0.20-}$	0.20	43	215
$Li_{0.04}^+(NH_4^+)_{0.18}(NH_3)_{0.43}TiS_2^{0.22-}$	0.22	46	209
$Li_{0.08}^+(NH_4^+)_{0.14}(NH_3)_{0.48}TiS_2^{0.22-}$	0.22	49	223
$Li_{0.11}^+(NH_4^+)_{0.11}(NH_3)_{0.50}TiS_2^{0.22-}$	0.22	49	223
$Li_{0.20}^+(NH_4^+)_{0.02}(NH_3)_{0.57}TiS_2^{0.22-}$	0.22	47	214
$Li_{0.20}^+TiS_2^{0.20-}$	0.20	41	205

[a] y'' has an experimental error of ± 0.04.

[b] χ_P has an experimental error of $\pm 4 \times 10^{-6}$ emu/mole.

[c] $\chi_P' = \chi_P/(x + y')$.

The observation that χ_P' is independent of the nature of the intercalant supports the validity of the rigid-band model for these materials. The independence of χ_P' as the NH_3 content is varied indicates that charge transfer from NH_3 to the TiS_2 host is negligible, which invalidates previous molecular-orbital (*5*) and Mulliken charge-transfer (*34*) treatments of the charge transfer process. Instead, charge transfer is accomplished by ionization of Li to Li^+ as well as oxidation of NH_3 to NH_4^+ if $x \lesssim 0.22$.

Conclusions

In this work we have demonstrated that the Li–NH_3 intercalates of TiS_2 are best described by the ionic formulation $Li_x^+(NH_4^+)_{y'}(NH_3)_{y''}TiS_2^{(x+y')-}$ for $0 \leq x \leq 0.20$. Although we cannot rule out the possibility that decomposition products such as hydride and NH_2^- may also intercalate into TiS_2, we have not been able to detect them. Furthermore, cationic charge compensation occurs such that 0.22 ± 0.02 mole of electrons per mole of TiS_2 are always transferred to the TiS_2 conduction band to satisfy the electronic requirements of the host. We believe that the observed charge compensation is related to the kinetics of the intercalation process. Since Li intercalates rapidly ($\lesssim$1 min) compared to NH_3 ($\simeq$ 2 hr), it follows that Li^+ enters the VDW gap well ahead of NH_4^+ or NH_3. Hence, the host has already received the valence electron of Li prior to capturing the electron associated with the formation of NH_4^+. This intercalation mechanism provides a simple explanation of the charge-compensation phenomenon in these compounds, since according to this mechanism NH_4^+ formation should occur only to an extent sufficient to transfer a total of 0.22 mole of electrons per mole of TiS_2 to the conduction band. If the situation were reversed, i.e., NH_3 intercalated much faster than Li, then 0.22 mole of NH_4^+ per mole of TiS_2 would be found consistently. Reversing this argument, it follows that the observation of charge compensation rein-

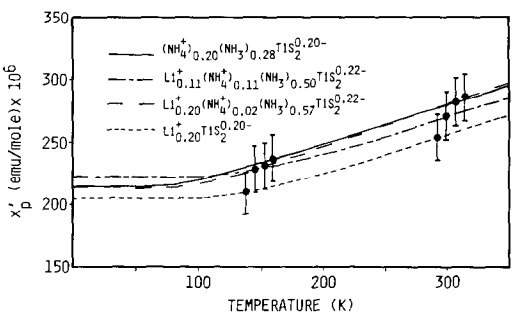

FIG. 6. A comparison of the susceptibility per mole of cation, $\chi_P' = \chi_P/(x + y')$, for $(NH_4^+)_{0.20}(NH_3)_{0.28}TiS_2^{0.20-}$, $Li_{0.11}^+(NH_4^+)_{0.11}(NH_3)_{0.50}TiS_2^{0.22-}$, $Li_{0.20}^+(NH_4^+)_{0.02}(NH_3)_{0.57}TiS_2^{0.22-}$, and $Li_{0.20}^+TiS_2^{0.20-}$. The experimental uncertainty in χ_P is $\pm 4 \times 10^{-6}$ emu/mole.

forces the proposed intercalation mechanism. Also, for metals that intercalate at rates comparable to that of NH_3, such as Eu, it may be possible to compare the relative intercalation rates of M and NH_3 by measuring the $M^+ : NH_4^+$ ratio (*35*).

This research has set the stage for the controlled synthesis of $M_x^+(NH_4^+)_{y'}(NH_3)_{y''}TiS_2^{(x+y')-}$ by both conventional and ion-exchange methods. The synthesis of these materials is currently under investigation in our laboratories.

Acknowledgment

The authors acknowledge the Magnetism and Magnetic Resonance Facility at Arizona State University for use of the SQUID magnetometer.

References

1. See, for example, the following excellent surveys: (*a*) F. R. GAMBLE AND T. H. GEBALLE, *in* "Treatise on Solid State Chemistry" (N. B. Hannay, Ed.), Vol. 3, p. 89, Plenum, New York, 1976; (*b*) M. S. WHITTINGHAM, *Prog. Solid State Chem.* **12,** 41 (1978); (*c*) F. A. LEVY, Ed., "Intercalated Layered Materials," Reidel, Dordrecht, 1979; (*d*) M. S. DRESSELHAUS AND G. DRESSELHAUS, *Adv. Phys.* **30,** 139 (1981); (*e*) S. A. SOLIN, *Adv. Chem. Phys.* **49,** 455 (1982); (*f*) M. S. DRESSELHAUS, *Phys. Today,* p. 60, March 1984.
2. A. D. YOFFE, *Solid State Ionics* **9/10,** 59 (1983).
3. A. D. YOFFE, *Annu. Rev. Mat. Sci.* **3,** 147 (1973).
4. F. R. GAMBLE, J. H. OSIECKI, M. CAIS, R. PISHARODY, F. J. DISALVO, AND T. H. GEBALLE, *Science* **174,** 493 (1971).
5. F. R. GAMBLE AND B. G. SILBERNAGEL, *J. Chem. Phys.* **63,** 2544 (1975).
6. R. SCHÖLLHORN AND H. D. ZAGEFKA, *Angew. Chem. Int. Ed. Engl.* **16,** 199 (1977).
7. L. BERNARD, M. MCKELVY, W. GLAUNSINGER, AND P. COLOMBET, *Solid State Ionics* **15,** 301 (1985).
8. J. DUNN AND W. S. GLAUNSINGER, unpublished results.
9. M. S. WHITTINGHAM, *J. Solid State Chem.* **29,** 303 (1979).
10. B. G. SILBERNAGEL AND M. S. WHITTINGHAM, *J. Chem. Phys.* **64,** 3670 (1976).
11. L. BERNARD, W. GLAUNSINGER, AND P. COLOMBET, *Solid State Ionics* **17,** 81 (1985).
12. R. L. KLEINBERG AND B. G. SILBERNAGEL, *Solid State Commun.* **36,** 345 (1980).
13. A. H. THOMPSON, *Phys. Rev. Lett.* **40,** 1511 (1978).
14. A. H. THOMPSON, *J. Electrochem. Soc.* **126,** 608 (1979).
15. J. R. DAHN AND R. R. HAERING, *Solid State Commun.* **40,** 245 (1981).
16. J. R. DAHN, D. C. DAHN, AND R. R. HAERING, *Solid State Commun.* **42,** 179 (1982).
17. J. R. DAHN AND R. R. HAERING, *Can. J. Phys.* **61,** 1093 (1983).
18. W. R. MCKINNON AND R. R. HAERING, *in* "Modern Aspects of Electrochemistry, No. 15" (R. E. White, J. O. M. Brockris, and B. E. Conway, Eds.), p. 235, Plenum, New York, 1983.
19. W. RÜDORFF, *Chimia* **19,** 489 (1965).
20. A. LEBLANC, Thesis, University of Nantes, 1975.
21. G. V. SUBBA RAO, M. W. SHAFER, AND L. J. TAO, *Mat. Res. Bull.* **8,** 1231 (1973).
22. See, for example, W. S. GLAUNSINGER, R. B. VON DREELE, R. F. MARZKE, R. C. HANSON, P. CHIEUX, P. DAMAY, AND R. CATTERALL, *J. Phys. Chem.* **88,** 3860 (1984).
23. "Preparation and Crystal Growth of Materials with Layered Structures" (R. M. A. Lieth, Ed.), Reidel, Dordrecht, 1977.
24. A. H. THOMPSON, U.S. Patent 4,069,301 (1978).
25. J. BEAR AND K. F. MCTAGGERT, *Aust. J. Chem.* **11,** 458 (1958).
26. A. H. THOMPSON, F. R. GAMBLE, AND C. R. SYMON, *Mat. Res. Bull.* **10,** 915 (1975).
27. R. R. CHIANELLI, J. C. SCANLON, M. S. WHITTINGHAM, AND F. R. GAMBLE, *Inorg. Chem.* **14,** 1691 (1975).
28. B. G. SILBERNAGEL, M. B. DINES, F. R. GAMBLE, L. A. GEBHARD, AND M. S. WHITTINGHAM, *J. Chem. Phys.* **65,** 1906 (1976).
29. K. JONES, *in* "Comprehensive Inorganic Chemistry" (J. C. Bailar, Jr., *et al.*, Eds.), Vol. 2, p. 244, Pergamon, Elmsford, N.Y., 1974.
30. M. S. WHITTINGHAM AND A. H. THOMPSON, *J. Chem. Phys.* **62,** 1588 (1975).
31. M. DANOT, L. LEBLANC, AND J. ROUXEL, *Bull. Soc. Chim. France,* 2670 (1969).
32. D. W. MURPHY, F. J. DISALVO, G. W. HULL, AND J. V. WASZCZAK, *Inorg. Chem.* **15,** 17 (1976).
33. W. S. GLAUNSINGER, S. ZOLOTOV, AND M. J. SIENKO, *J. Chem. Phys.* **56,** 4756 (1972).
34. J. V. ACRIVOS, S. F. MEYER, AND T. H. GEBALLE, "Colloque Weyl III" p. 341, Springer, New York, 1973.
35. S. P. HSU, Ph.D. Thesis, Arizona State University, 1985.